ChemComm

COMMUNICATION

View Article Online
View Journal | View Issue

Cite this: *Chem. Commun.*, 2019, **55**, 3215

Received 11th December 2018,
Accepted 19th February 2019

DOI: 10.1039/c8cc09818b

rsc.li/chemcomm

Perfluoroalkane wax infused gels for effective, regenerating, anti-icing surfaces†

Arun Sandhu, [a] Oliver J. Walker,[a] Andrés Nistal, [a] Kwang Leong Choy*[a] and Adam J. Clancy *[ab]

Infusion of solid perfluoroalkanes into polydimethylsiloxane gels provides a simple route to regenerating deicing surfaces, with low adhesion strength from the lower inherent cohesive energy of the perfluoroalkanes. Further, these surfaces are more hydrophobic and environmentally stable than their alkane analogues. The result is a robust, regenerating surface which demonstrates low energy ice adhesion (19.6 kPa), hydrophobicity (water contact angle, CA, >100°), and high environmental stability.

While there is broad agreement in the need for anti-icing surfaces for many applications such as aeronautics, marine, and consumer goods, there is disagreement of how such properties should be achieved.[1] Icephobicity can be accomplished by preventing the formation of ice (anti-icing) through the use of hydrophobic (CA, >90°) surfaces,[2] limiting water/surface contact time to minimise ice accretion. These surfaces are typically low energy, allowing icephobicity to be imbued by minimising ice adhesion strength (IAS), with sufficiently low values[3] leading to passive ice sloughing (deicing),[4] although the relationship between hydrophobicity and IAS is still the subject of some debate.[5–7] Superhydrophobic surfaces (CA >150°) provide greater hydrophobicity, typically utilising the 'lotus-leaf effect' through use of nanorough structures from etching of a surface,[8] deposition/growth of nanoscale species,[9] or well controlled, lithographic hierarchical structures.[10] These superhydrophobic surfaces are highly anti-icing[11,12] as liquid water contact time is dramatically lower than simple hydrophobic surfaces. However, upon the formation of ice, deicing may be complicated by the increased effective surface area of superhydrophobic systems increasing the total ice-surface adhesion force.[13] As an alternative route to hydrophobicity and icephobicity, liquid lubricants may be infused into a porous surface[14] to provide a regenerating, smooth, so-called Slippery Liquid-Infused Porous Surface (SLIPS).[15] These systems are superhydrophobic and may deice at low strengths[3,16,17] (≤20 kPa, with extremes of 0.2 kPa seen) with the liquid preventing water penetration to the underlying, high surface area, textured solid. SLIPS provide greater scalability than the superhydrophobic lithographic structures, and improved performances over simple rough surfaces and are a promising route towards scalable manufacture of omniphobic, self-cleaning materials. However, the rate and repeatability of regeneration has been questioned,[18,19] while their fragility to even mild mechanical abrasion is inherent due to the soft nature of the components. Meanwhile, the surface liquid poses issues regarding lifetime, potentially with significant environmental issues from contamination in real-world applications. The leeching of the liquid can occur through several routes: contact with the surface (exacerbated by capillary action), sacrificial removal alongside removed contaminants during cleaning, miscibility in environmental water (*e.g.* rain), and evaporation. Some 'smart' SLIPS systems facilitate switching between liquid and a more robust solid state using a thermal[20] or photonic trigger,[21] although water mobility is only seen in the liquid state.

Due to these issues, alternative mechanically robust icephobic materials are still of much interest, such as the recently developed interfacial-slipping partial crosslinked elastomers,[3] and alkane infused gels[22] (AIG). AIGs involve infusing a surface-bound material into a storage reservoir akin to SLIPS, however, in contrast to a textured surface used to store liquid infusant, with AIGs, a melted alkane wax is infused into a bulk crosslinked polymer to create an all-solid-state swollen gel, with wax diffusing to the surface as a thin coating. The mechanical properties of the AIGs are superior to SLIPS and many nanostructured superhydrophobic surfaces, while eliminating the infusant loss from evaporation and wicking. While hydrophobic, AIGs do not have CAs in the superhydrophobic regime, however, contaminants (*e.g.* ice) can be removed with minimal force (<100 kPa), attributed to a stripping away of the surface layer of alkane. The broken bonds are thought to be the weak intramolecular alkane bonds with a 'sacrificial' layer removed

[a] *Institute for Materials Discovery, University College London, WC1E 7JE, UK. E-mail: k.choy@ucl.ac.uk*
[b] *Department of Chemistry, University College London, WC1E 7JE, UK. E-mail: a.clancy@ucl.ac.uk*

† Electronic supplementary information (ESI) available. See DOI: 10.1039/c8cc09818b

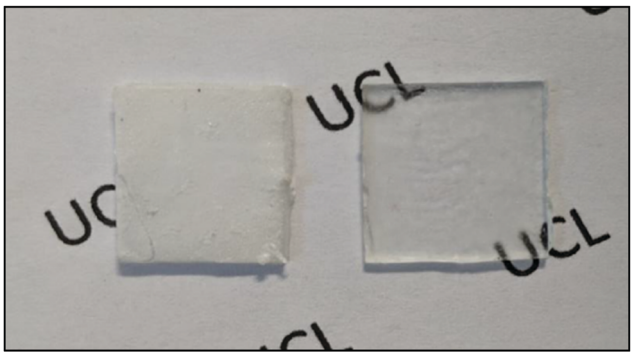

Fig. 1 Digital photograph of PIGs from infused C14F (left) and C9F (right). Samples 1.5 cm across.

along with the ice/contaminant. The removed surface layer spontaneously regenerates due to internal stress of the swelled gel network on infused alkanes, forcing it to the surface, facilitating solid-state diffusion.

Here, AIGs are improved by incorporation of the perfluoroalkanes (PFAs) as infusion agents to improve the intrinsic properties of these infused solids. PFAs (unbranched and of the form C_nF_{n+2}, here termed C*n*F) have weaker cohesive energies than their alkane (C_nH_{n+2}, unbranched, termed C*n*H) counterparts,[23] allowing more facile deicing in this system. The inherent hydrophobicity of PFA and perfluorinated surfaces compared to alkanes concurrently improves anti-icing mechanism, with the increased contact angles limiting water contact time and surface-water cross-sectional area. Furthermore, the virtually zero solubility of PFAs in water[24] may reduce the rate of passive leeching of wax into the environment.

To test the potential of PFA infused gels (PIGs, Fig. 1), they were compared to the AIGs. Waxes to be infused required melting points (ESI,† Fig. S1) above room temperature, but low enough for simple heating to facilitate processing (<*ca.* 100 °C). The PFAs C9F (m.p. −16 °C), C10F (36 °C), C12F (75 °C) and C14F (103 °C) were selected (C11F and C13F were not commercially available). For controls, wax alkanes C17H (21 °C), C19H (31 °C) and C24H (49 °C) were used. Polydimethylsiloxane (PDMS, Sylgard 184) was mixed manually, centrifuged to remove bubbles (3500*g*, 2 min), cast as a 200 μm layer on glass slides, and cured 48 h at room temperature. The gels were submerged in a 150 °C bath for 4 h, except for C9F which used a lower temperature (105 °C) to keep the PFA well below the boiling point (125 °C). Samples were removed from the bath and cooled to room temperature, forming distinct organic coatings on the surface: the low molecular weight C9F and C17H showed a transparent coating at the surface, akin to classic SLIPS, while all others formed a wax-like opaque frosting at the surface (Fig. 1).

While the low cohesive energy and associated omniphobicity/universal immiscibility of PFAs may have been thought to be a potential barrier to infusion, full infusion of even the heaviest and least mobile PFA into the gel can be seen through scanning electron microscopy/electron dispersive X-ray spectroscopy (SEM-EDS, Fig. 2). The glass and PDMS layers can be identified

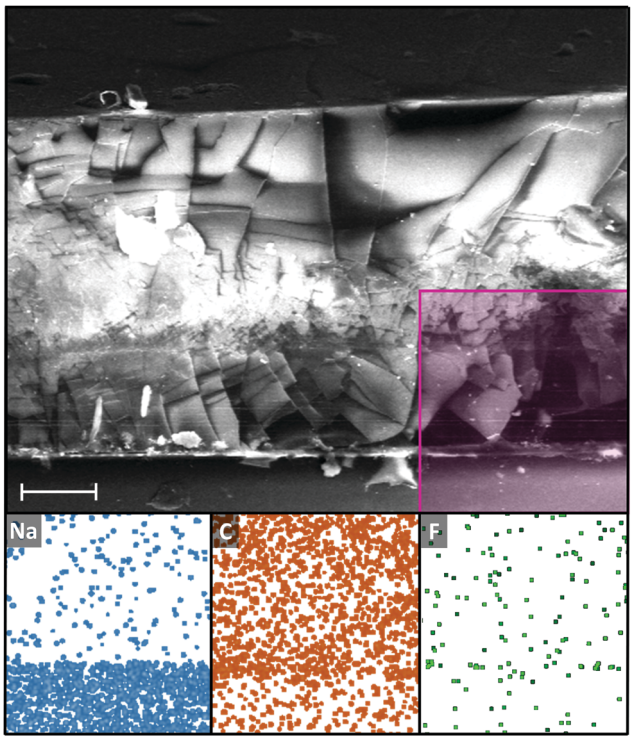

Fig. 2 SEM (top) and EDS maps (bottom, from left to right, sodium, carbon, fluorine) of C14F PIG cryofracture cross-section. Shaded area in SEM indicates location of EDS map. Additional SEM supplied in ESI† (Fig. S2). Heterogeneity of the film structure in the cross-section is attributed to the cryofracture procedure. Scale bar 50 μm.

through EDS of sodium (from soda-lime glass substrate) and carbon (from PDMS and infused PFA), with an even fluorine signal seen down to the bottom of the gel.

IASs were tested through transverse shear applied to a column of ice on the substrate surface by a force transducer at −10 °C (full details supplied in the ESI†). Both AIGs and PIGs showed a dramatic reduction of the IAS compared to the pure PDMS (Fig. 3a); it should be noted that PDMS (108 kPa) is already an effective and commonly used icephobic coating.[25] The PIGs showed reasonably consistent values (31.7–19.6 kPa), with a broad trend of lower molecular weights providing lower IASs, as might be expected from the longer molecules having stronger van der Waals forces and thus cohesive energies. It is worth noting that the adhesion strength of the 'liquid' (at −10 °C) infused CF9 PIG is not substantially different to the 'solid' infused CF10, as seen previously in the AIGs.[22] The IASs of AIGs were consistent with previous literature,[22] and higher than PIGs. The correlation with molecular weight was also seen, with the smallest tested molecules showing values comparable to the PIGs (C17H, 26.3 kPa), however, the larger C24H showed a significantly higher adhesion (73.1 kPa), albeit still below the commonly used 100 kPa threshold of 'icephobic'.[26] Measurement of IAS on the constituent waxes (ESI,† Fig. S4) showed wax cohesive failure occurs before ice/wax adhesive failure (ESI,† Fig. S5 and S6), with PFA deicing showing similar values to the respective PIGs, indicating deicing occurs through cohesive failure of the wax. Conversely, alkane cohesive strengths (145–240 kPa) are

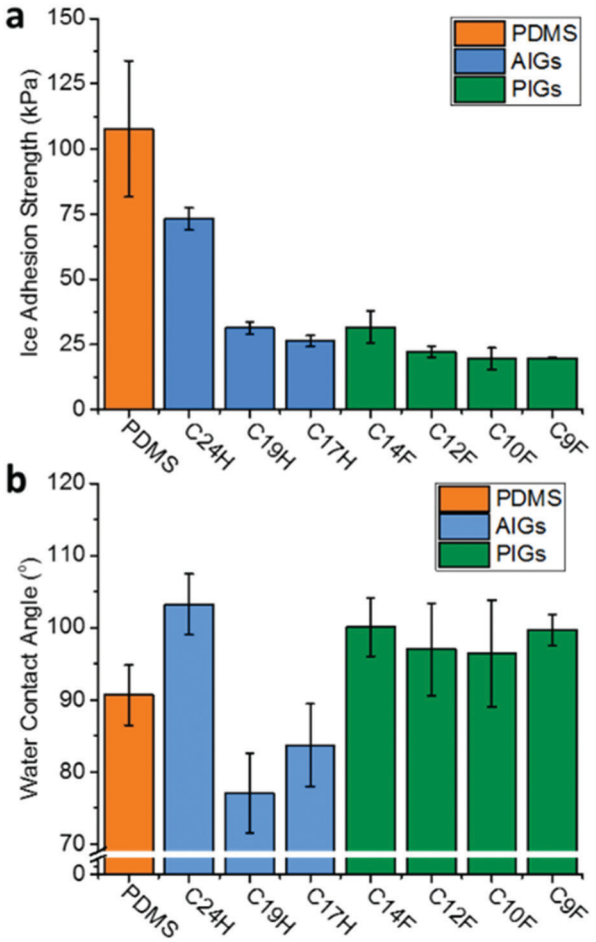

Fig. 3 (a) Ice adhesion strength and (b) sessile water contact angle of perfluoroalkane/alkane infused and uninfused PDMS gel.

substantially higher than the AIG's IAS, so deicing of AIGs is attributed to adhesive failure of the alkane/PDMS interface.

As expected from the high intrinsic hydrophobicity PFAs, the water contact angle (CA) of the PIGs showed an increase in hydrophobicity (Fig. 3b, CA 96.5°–100.1°) compared to the neat PDMS surface (90.7°), making it more suitable as a protective hydrophobic coating. These values appear broadly independent of molecular length, and lower than the pure PFAs (*ca.* 116°, ESI,† Fig. S4). In contrast, the lighter-alkane infused gels show a lessening of CA (77.1°–83.7°) compared to the PDMS, as might be expected given the already intrinsically hydrophobic nature of PDMS. The heavy C24H actually demonstrated the highest hydrophobicity (103.2°), however, this is coupled to the previously established poor icephobicity.

One of the most important benefits of the previously produced alkane infused gels was the possibility of regeneration of the alkane layer (similar to the regeneration of liquids in SLIPS). Here, the regeneration was demonstrated through manual removal of the surface PFA layer, with the surface monitored by reflectance optical microscopy (Fig. 4). Initially, the sample shows a bare surface, missing the characteristic domains of wax seen on the surface of solid PFA, indicating that the PDMS surface is visible. After 4 h, wax domains tens of microns across can be seen to have

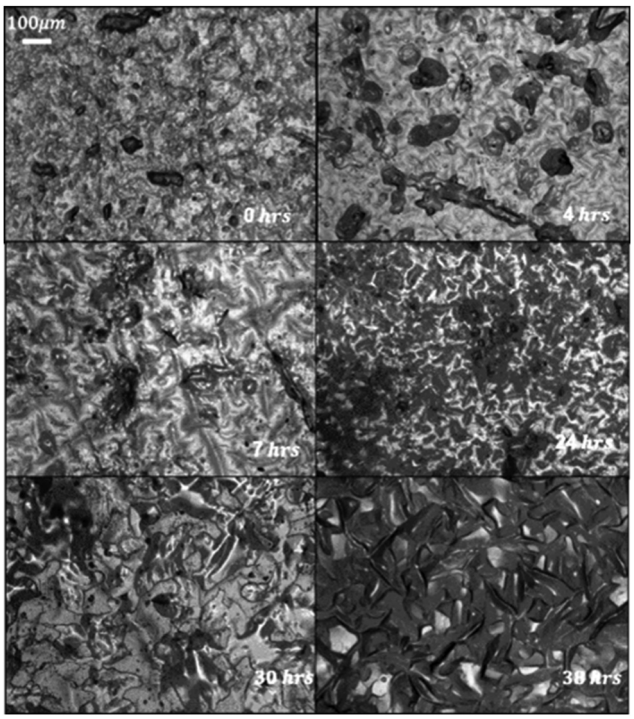

Fig. 4 Regeneration of wiped C12F surface over from (top left to bottom right) 0, 4, 7, 24, 30 and 38 h.

recovered, and the surface continues maturing with expanding islands until the surface is covered by ~24 h and the domains stop coalescing after ~30 h.

Finally, there is a concern with using materials with labile components in environmental applications, particularly as icephobic coatings are typically used for weather protection, thus exposed to the environment. It should be noted that PFAs show even higher environmental persistence than alkanes[27] due to their resistance to photolysis, hydrolysis, and biodegradation, however, environmental hazard from linear alkanes is also well established.[28–30] While some environmental loss may be expected from adhesion to ice in any SLIPS or infused gel system, the use of a solid infusant will virtually remove vapour loss, and the greatest risk to leeching is though water. To test passive leeching of the infused alkane in marine applications, gels were soaked in stirring synthetic sea water[31] for five 24 h periods, with the water tested for contaminants by gas chromatography-mass spectrometry (GC-MS) afterwards (ESI,† Fig. S7 and S8). The C9F PIG and C19H AIG were selected for testing; C19H showed low, but clearly measurable solubility of the neat alkane (ESI,† Fig. S7), and the AIG showed clear peaks in the signal for aliquots taken for the first 2 days, at corresponding times to the alkane control (with signal sufficiently strong to measure MS of $C_{19}H_{40}$ for the day 1 aliquot). It is assumed that the surface alkane layer slowly dissolved over 2 days, while the infused hydrophobic alkane remained in the hydrophobic PDMS gel network rather than become exposed to the water by forming a new (sparingly soluble) surface layer. Conversely, the PIG in water (ESI,† Fig. S8) showed no any evidence of dissolution of the infused organic at any point, with no detectable dissolution after 2 weeks of soaking, as might

be expected due to the increased hydrophobicity seen for the PIGs (Fig. 3b).

In conclusion, the use of perfluoroalkanes in lieu of alkanes for infusion into gels has been shown to improve their properties for the formation of a sacrificial organic layer for icephobicity and cleanablility. The PFAs are capable of complete diffusion into the gels in spite of their lower surface energies, allowing the swollen gel architecture to be achieved, and their greater omniphobicity and weaker intermolecular bonding facilitates low ice adhesion strengths (19.6 kPa). The increased hydrophobicity of the perfluoroalkanes provides the additional benefits of increased water repulsion (limiting water contact and reducing ice accretion), and reduced solubility in water, dramatically reducing passive leeching from the gels into water.

This research was funded in part by the European Commission (SEDNA: Safe maritime operations under extreme conditions: the Arctic case, project 723526).

Conflicts of interest

The authors declare no competing financial interest.

References

1 M. J. Kreder, J. Alvarenga, P. Kim and J. Aizenberg, *Nat. Rev. Mater.*, 2016, **1**, 15003.
2 S. Kulinich and M. Farzaneh, *Appl. Surf. Sci.*, 2009, **255**, 8153–8157.
3 K. Golovin, S. P. Kobaku, D. H. Lee, E. T. DiLoreto, J. M. Mabry and A. Tuteja, *Sci. Adv.*, 2016, **2**, e1501496.
4 H. Sojoudi, H. Arabnejad, A. Raiyan, S. A. Shirazi, G. H. McKinley and K. K. Gleason, *Soft Matter*, 2018, **14**, 3443–3454.
5 Z. A. Janjua, B. Turnbull, K.-L. Choy, C. Pandis, J. Liu, X. Hou and K.-S. Choi, *Appl. Surf. Sci.*, 2017, **407**, 555–564.
6 A. J. Meuler, J. D. Smith, K. K. Varanasi, J. M. Mabry, G. H. McKinley and R. E. Cohen, *ACS Appl. Mater. Interfaces*, 2010, **2**, 3100–3110.
7 M. Nosonovsky and V. Hejazi, *ACS Nano*, 2012, **6**, 8488–8491.
8 L. B. Boinovich, A. M. Emelyanenko, V. K. Ivanov and A. S. Pashinin, *ACS Appl. Mater. Interfaces*, 2013, **5**, 2549–2554.
9 D. K. Sarkar and M. Farzaneh, *J. Adhes. Sci. Technol.*, 2009, **23**, 1215–1237.
10 T. Liu and C.-J. Kim, *Science*, 2014, **346**, 1096–1100.
11 Y. Tang, Q. Zhang, X. Zhan and F. Chen, *Soft Matter*, 2015, **11**, 4540–4550.
12 C. Wei, B. Jin, Q. Zhang, X. Zhan and F. Chen, *J. Alloys Compd.*, 2018, **765**, 721–730.
13 M. J. Kreder, J. Alvarenga, P. Kim and J. Aizenberg, *Nat. Rev. Mater.*, 2016, **1**, 15003.
14 C. Urata, G. J. Dunderdale, M. W. England and A. Hozumi, *J. Mater. Chem. A*, 2015, **3**, 12626–12630.
15 T.-S. Wong, S. H. Kang, S. K. Tang, E. J. Smythe, B. D. Hatton, A. Grinthal and J. Aizenberg, *Nature*, 2011, **477**, 443.
16 G. Zhang, Q. Zhang, T. Cheng, X. Zhan and F. Chen, *Langmuir*, 2018, **34**, 4052–4058.
17 P. Kim, T.-S. Wong, J. Alvarenga, M. J. Kreder, W. E. Adorno-Martinez and J. Aizenberg, *ACS Nano*, 2012, **6**, 6569–6577.
18 S. B. Subramanyam, K. Rykaczewski and K. K. Varanasi, *Langmuir*, 2013, **29**, 13414–13418.
19 J. Cui, D. Daniel, A. Grinthal, K. Lin and J. Aizenberg, *Nat. Mater.*, 2015, **14**, 790.
20 K. Manabe, T. Matsubayashi, M. Tenjimbayashi, T. Moriya, Y. Tsuge, K.-H. Kyung and S. Shiratori, *ACS Nano*, 2016, **10**, 9387–9396.
21 J. Wang, W. Gao, H. Zhang, M. Zou, Y. Chen and Y. Zhao, *Sci. Adv.*, 2018, **4**, eaat7392.
22 Y. Wang, X. Yao, S. Wu, Q. Li, J. Lv, J. Wang and L. Jiang, *Adv. Mater.*, 2017, **29**, 1700865.
23 A. Maciejewski, *J. Photochem. Photobiol., A*, 1990, **51**, 87–131.
24 J. G. Riess, *Chem. Rev.*, 2001, **101**, 2797–2920.
25 H. Jellinek, H. Kachi, S. Kittaka, M. Lee and R. Yokota, *Colloid Polym. Sci.*, 1978, **256**, 544–551.
26 H. Sojoudi, M. Wang, N. Boscher, G. McKinley and K. Gleason, *Soft Matter*, 2016, **12**, 1938–1963.
27 R. C. Buck, J. Franklin, U. Berger, J. M. Conder, I. T. Cousins, P. De Voogt, A. A. Jensen, K. Kannan, S. A. Mabury and S. P. van Leeuwen, *Integr. Environ. Assess. Manage.*, 2011, **7**, 513–541.
28 C. Lintas, A. Balduzzi, M. Bernardini and A. Di Muccio, *Lipids*, 1979, **14**, 298–303.
29 P. Souza-Alonso, L. González and C. Cavaleiro, *J. Chem. Ecol.*, 2014, **40**, 1051–1061.
30 E. Bingham, B. Cohrssen and C. H. Powell, *Patty's toxicology. Volume 3: metals and metal compounds, compounds of inorganic nitrogen, carbon, oxygen and halogens*, 2001.
31 D. R. Kester, I. W. Duedall, D. N. Connors and R. M. Pytkowicz, *Limnol. Oceanogr.*, 1967, **12**, 176–179.

